THE STABILITY OF PISCES IV

by

G. V. Parkinson, P. Eng.

AN INVESTIGATION OF THE STABILITY OF PISCES IV

by

G.V. Parkinson, P. Eng.

for the

Marine Sciences Directorate
Department of the Environment

October, 1974

SUMMARY

A 1/8- scale model of the submersible Pisces IV was tested in a wind tunnel of the department of mechanical engineering at the University of British Columbia. The original configuration of the model was found to be unstable in pitch and yaw, and the measurements were used to explain the pitch oscillations and severe speed limitations caused by control problems observed in the submersible on a trial run. Two sets of horizontal and vertical tail fins were designed, built, and tested on the model, and the larger set, plus the calculated augmentation of the thruster slipstreams acting on the horizontal fins, are predicted to provide satisfactory stability and control. It is recommended that the submersible be equipped with these larger fins.

TABLE OF CONTENTS

LIST OF FIGURES

NOMENCLATURE

A	–	projected frontal area of submersible; reference area
d	=	$\sqrt{A}$ - reference length
C	–	chord of fin
ℓ	–	distance from line of action of lift force on fin to submersible centre of gravity
A_F	–	planform area of pair of horizontal or vertical fins
d_j	–	diameter of jet from thruster
$A_j = \frac{\pi}{4} d_j^2$	–	cross-sectional area of jet
G	–	position of submersible centre of gravity
B	–	position of submersible centre of buoyancy
$\overline{BG}$	–	distance from G to B
α	–	angle of attack of submersible, referred to deck
$\dot{\alpha} = \frac{d\alpha}{dt}$	–	pitch angular velocity
$\ddot{\alpha} = \frac{d^2\alpha}{dt^2}$	–	pitch angular acceleration
t	–	time
β	–	angle of yaw of submersible
δ_H	–	deflection angle of horizontal fins
δ_V	–	deflection angle of vertical fins
ρ	–	fluid mass density
μ	–	fluid dynamic viscosity
V	–	speed of submersible, or speed of air in wind tunnel
$R_e = \frac{\rho V d}{\mu}$	–	Reynolds number of submersible
$q = \frac{\rho}{2} V^2$	–	dynamic pressure of flow
V_j	–	velocity of jet from thruster
$q_j = \frac{\rho}{2} V_j^2$	–	dynamic pressure of jet

L	-	lift force on submersible
D	-	drag force on submersible
S	-	side force on submersible
M	-	pitching moment about G on submersible
Y	-	yawing moment about G on submersible
F	-	lift force on pair of horizontal or vertical fins
$C_L = \frac{L}{qA}$	-	lift coefficient of submersible
$C_D = \frac{D}{qA}$	-	drag coefficient of submersible
$C_S = \frac{S}{qA}$	-	side force coefficient of submersible
$C_M = \frac{M}{qAd}$	-	pitching moment coefficient of submersible
$C_Y = \frac{Y}{qAd}$	-	yawing moment coefficient of submersible
$C_F = \frac{F}{qA_F}$	-	lift coefficient for pair of horizontal or vertical fins
W	-	weight of submersible
F_B	-	buoyant force of submersible
T	-	thrust of one thruster
B.H.P.	-	brake horsepower of both thrusters
η	-	propulsive efficiency of thrusters
θ	-	period of pitch oscillation
ζ	-	damping factor of pitch oscillation
Δ	-	increment in a quantity
T_C	-	thrust coefficient, defined in text

1. INTRODUCTION

In order to perform satisfactorily in the missions planned for her, the submersible Pisces IV must be able to fly a straight and level course at a speed of from one to two knots while submerged. She cannot do this in her present configuration, because the basic hull shape, if given a small angular displacement in pitch (the vertical plane of symmetry) or yaw (the horizontal plane), while moving forward through the water, experiences hydrodynamic torques which tend to turn the hull broadside.

In pitch, there is a counter-acting hydrostatic torque from the couple of weight and buoyant force, so that the resulting vessel motion is a slow pitch oscillation, which may be persistent and of considerable amplitude, since damping torques are small. In yaw, the vessel continually drifts off course. To combat these deviations from course, the pilot has control of two thrusters. These can provide yaw control by differential thrust, but are ineffective for pitch control, even though they can be tilted about a horizontal transverse axis, because the vessel center of gravity is nearly on the tilt axis and the thrust line.

An alternative method of controlling, and indeed stabilizing the vessel in pitch and yaw would be to provide moveable horizontal and vertical fins at or near the stern, as with naval submarines or, in the aeronautical analogue, with dirigibles. The purpose of the present investigation was to design and wind-tunnel test a satisfactory set of horizontal and vertical fins for Pisces IV.

2. EXPERIMENTAL METHODS

2.1 The Test Model A 1/8- scale model of Pisces IV was supplied by the Marine Sciences Directorate. The model had the thrusters incorrectly

located too far aft, and did not include the manipulators and various other protuberances from the front part of the hull, but was otherwise assumed to be an accurate replica of the submersible. Neither of the above discrepancies would have an important effect on the results - in fact, the thruster units were removed from the model for the tests with fins added, since, in the absence of the jets the thrusters produce under power (there was of course no provision for this in the model tests) they are merely drag-producing devices which would have degraded the flow over the horizontal fins.

The two sets of horizontal and vertical fins tested were made of wood, and mounted in pairs on steel shafts. The horizontal shaft had a pitch arm inside the hull on the model centre-line, which protruded from the stern and engaged a sector plate, so that pitch angles of the horizontal fins could be set in increments of 1° between $\pm 5°$. The vertical shaft had a yaw arm lying forward along the deck, where it also engaged a sector plate, so that yaw angles of the vertical fins could be set in increments of 2° between $\pm 6°$.

The model with the second and final set of fins mounted is shown in the wind tunnel in Figs. 1 and 2.

2.2 The Wind Tunnel The tests were carried out in the closed-circuit wind-tunnel of the department of mechanical engineering at the University of British Columbia. The test section is 36 inches wide by 27 inches deep by 104 inches long, and has a uniform flow with a turbulence level of less than 0.1°/$_o$ and a speed range of 5 to 100 mph. It is equipped with a 6-component strain gauge balance. The test model is mounted on the balance turntable, which can be yawed through 360°, by struts which pass

through a dummy turntable in the test section floor.

With the 3-strut mounting shown in Figs. 1 and 2, the model can be given positive or negative angles of pitch (called angles of attack in aerodynamics) by the rotation of a crank hinged to the tail mounting strut. This mounting was used for all tests in which angle of attack was varied, and for the test of the basic model configuration at angles of yaw. An alternative 2-strut mounting was used for all other tests at angles of yaw, when the yaw performance in preliminary tests of the first set of vertical fins proved unsatisfactory, and the tail mounting strut was removed in case its wake was contributing to the poor fin performance. In this 2-strut mounting, cantilever brackets are rigidly attached to the 2 front mounting struts, and the model is mounted on them. In both mountings, these front mounting struts are shielded from the wind by fairings, so that the struts do not contribute to the aerodynamic loads measured by the balance.

2.3 The Tests The full scale Pisces IV, flying steadily at reasonably deep submergence in sea water, and the model, hold stationary in the wind tunnel in a uniform incident air stream, experience dynamically similar flows, so that the forces and torques (or moments, in aerodynamics) on the prototype can be predicted from the tests on the model, if the following criteria are met:

(i) The model must be an accurate scale model.

(ii) The Reynolds number R_e (this measures the ratio of inertial and viscous stresses in the flow and is defined in the Nomenclature.) must be the same for the two flows.

(iii) Corrections must be made to the wind tunnel data for the effects

of the presence of the mounting struts and the test section walls.

In the present tests, (i) is met adequately, with the exceptions noted in § 2.1. For (ii), the main test R_e was somewhat below the full-scale range because of wind tunnel power limitations, and would correspond to a speed of 0.8 kt. of the actual submersible. However, tests were conducted, with the model at zero angles of attack and yaw, to the full-scale equivalent of over 1 kt. For (iii), the necessary corrections were made by standard methods, and only the corrected data are presented in the report.

The test results are presented in the form of dimensionless coefficients of drag, lift, side force, pitching moment, and yawing moment C_D, C_L, C_S, C_M, and C_Y respectively, as functions of angle of attack α, angle of yaw β, horizontal and vertical fin deflection angles δ_H and δ_V, and Reynolds number R_e. These quantities are defined in Fig. 3 and in the Nomenclature. The following tests were performed:

(i) Basic configuration. Tunnel dynamic pressure q = 12.30psf. Measure C_D, C_L, C_M at $\beta = 0$, for $\alpha = -10°, -5°, 0, 5°, 10°$.

(ii) Basic configuration. q = 12.30psf. Measure C_D, C_S, C_Y at $\alpha = 0$, for $\beta = -10°, -5°, 0, 5°, 10°$.

(iii) Basic configuration. $\alpha = \beta = 0$. Measure C_D, C_L, C_M for q = 6.15, 12.30, 18.45, 21.53psf.

(iv) Model with first set of horizontal and vertical fins. $\delta_V = \delta_H = 0$. Otherwise same conditions as (i).

(v) Repeat (iv) with $\delta_H = -5°, -2°, +2°, +5°$.

(vi) Model with first set of horizontal and vertical fins. $\delta_V = \delta_H = 0$. Otherwise same conditions as (ii).

(vii) Repeat (vi) with $\delta_V = \pm 6°$.

(viii) Model with second set of horizontal and vertical fins, Repeat (iv), eliminating test at $\alpha = -10°$, because of tall upper vertical fin.

(ix) Repeat (viii) with $\delta_H = -2°, +2°$.

(x) Model with second set of horizontal and vertical fins. Repeat (vi).

(xi) Repeat (x) with $\delta_V = -6°, +6°$.

(xii) Model with second set of horizontal and vertical fins. Repeat (iii) for $q = 3.08, 6.15, 9.23, 12.30, 15.38, 18.45, 21.53$ psf.

3. CHARACTERISTICS OF THE BASIC CONFIGURATION

3.1 Characteristics in Pitch Figs. 4, 5, and 6 give the results of the tests of the model as it was received from the Marine Sciences Directorate (except for the removal of the propellers from the nacelles, and the addition of the small angle brackets attaching it to the mounting struts). Some model test results for this configuration were already available (Ref. 1), but they proved inadequate for the present purposes. What is needed is a detailed determination of the behaviour of Pisces IV in pitch, in yaw, and as a function of Reynolds number.

Fig. 4 gives the results of the tests of the model in pitch, presented as curves of C_D, C_L, and C_M as functions of α for $\beta = 0$, and for the test R_e corresponding to 0.8 kt. full scale. For all three curves the data vary smoothly and without appreciable scatter, and the trends agree qualitatively with the accepted behaviour for an approximately cylindrical body like Pisces IV. C_D has a minimum near $\alpha = 0$, and the value $C_D = 0.325$ at $\alpha = 0$ is typical of the class of body shape. C_L increases approximately linearly with α, and the slope of the curve

$\frac{dC_L}{d\alpha}$ at $\alpha = 0$ is +0.025 per degree, again reasonable for the shape.

The most important variation is that of C_M. It increases linearly with α, with a slope $\frac{dC_M}{d\alpha} = +0.020$ per degree. Thus, a small nose-up attitude of the submersible, while moving forward, produces a pitching moment which will cause the nose-up attitude to increase. The submersible is therefore said to be statically unstable in pitch, with respect to hydrodynamic pitching moments. However, this hydrodynamic tendency to rotate increasingly nose-up is counteracted, as mentioned in § 1, by a hydrostatic righting couple, and the resulting effects on the trim and stability of the vessel in pitch are analyzed in § 3.5 and 3.6. In connection with the trim, or equilibrium attitude of the vessel, it will be noted that at $\alpha = 0$ (deck level) there is a positive $C_M = +0.105$. This results from the effective negative camber of the hull shape.

3.2 Characteristics in Yaw Fig. 5 gives the results of the tests of the model in yaw, presented as curves of C_D, C_S, and C_Y as functions of β for $\alpha = 0$, and for the same R_e. The curves have qualitatively similar behaviour to those of Fig. 4, because there is not much difference between yaw and pitch to the roughly cylindrical hull shape. However, since the shape is symmetrical in plan form about a longitudinal axis, C_D is more nearly symmetric, and C_S and C_Y almost exactly antisymmetric, about $\beta = 0$.

The curve of C_S has a slope $\frac{dC_S}{d\beta} = +0.025$ per degree. Here the important variation is that of C_Y, and it is nearly linear with β, with slope $\frac{dC_Y}{d\beta} = \overset{+}{-}0.017$ per degree at $\beta = 0$. Again, the vessel is seen to be statically unstable in yaw. Here, however, there is no

counteracting hydrostatic effect, so the tendency of a small displacement in yaw to increase, with the vessel moving increasingly off course, would have to be corrected by differential thrust from the two thrusters.

3.3 Reynolds Number Characteristics The behaviour in pitch and yaw at values of R_e corresponding to the desired speed range of 1 to 2 knots of Pisces IV in sea water could not be explored in the wind tunnel because of power limitations, but at $\alpha = \beta = 0$ it was possible to test up to $R_e = 0.79(10)^6$, corresponding to 1.04 kts. full scale. The reason for anticipating that C_D, C_L, or C_M might change with increasing R_e is that the flow over a shape like that of Pisces IV is partially separated with a relatively broad wake, and the lines of flow separation on curved body surfaces are located by flow interactions which depend on R_e.

Fig. 6 gives the results of tests of the model at $\alpha = \beta = 0$, presented as curves of C_D and C_M as functions of R_e. C_L remained zero throughout the R_e-range tested. C_D and C_M show a decrease as R_e increases from the regular test value of $0.59(10)^6$ to $0.79(10)^6$. The decrease in C_D is less than 2°/₀, and in C_M about 11°/₀. The trends are in agreement with experience for similar shapes, and the results give confidence that carrying out the main test program at $R_e = 0.59(10)^6$ is satisfactory, since the actual pitching moments in the full-scale speed range will be somewhat less than those predicted from the model tests.

3.4 Speed Capability The C_D measurements of Fig. 6 provide the necessary data for a calculation of the maximum speed of Pisces IV, given its propulsive characteristics. These were given verbally to the author by Mr. J. McFarlane, the former director of engineering of

HYCO, the manufacturers of Pisces IV. It is powered by two propellers of 17 inches diameter, mounted in Kort nozzles (Ref. 2) and each powered by a 5 H.P.D.C. motor.

The maximum speed V_{max} is given by equating the power required to overcome the drag D_{max} to the power output available from the propellers:

$$D_{max}V_{max} = C_D \frac{\rho}{2} AV_{max}^3 = 550\,\eta\ \text{B.H.P.} \tag{3.1}$$

From Fig. 6, C_D can be estimated to level off at 0.325 for speeds above 1 kt. Also, ρ = 1.99 slug/cu.ft., A = 51.5 sq.ft, B.H.P. = 10.0. The ideal propulsive efficiency of the propellers in the Kort nozzles is estimated by simple momentum theory, according to which (see Ref. 2):

$$\eta = \frac{2}{1+ V_j/V} \tag{3.2}$$

and

$$\frac{V_j}{V} = \frac{1}{2} + \sqrt{\frac{1}{4} + \left(\frac{C_D A}{4A_j}\right)} \tag{3.3}$$

where V_j and A_j are the velocity and cross-sectional area of the jet discharging from one nozzle. Here A_j = 1.58 sq.ft., and substitution in Eqs. (3.3) and (3.2) gives (V_j/V) = 2.20 and η = 62.5°/₀. Therefore, from Eq. (3.1):

$$V_{max} = \left\{\frac{550(.625)10.0(2)}{.325(1.99)51.5}\right\}^{1/3} = 5.90 \text{ fps} = \underline{3.50} \text{ kts.}$$

Even if C_D were as high as 0.50, because of the protuberances from the surface of the full-scale hull, and if actual η were as low as 50°/₀, because of frictional effects, the submersible should still be capable of over 2.8 kts.

3.5 Trim Conditions For steady, unaccelerated horizontal motion through the water while submerged, the vessel must be in force and moment equilibrium. If it moves forward at β = 0, its symmetry gives $C_S = C_Y = 0$, as in Fig. 5, so lateral trim is achieved. For horizontal force

equilibrium the total thrust 2T from the two thrusters equals the drag D, assuming the thrust lines to be horizontal. For vertical force equilibrium, the weight W is balanced by the hydrodynamic lift L plus the hydrostatic buoyant force F_B:

$$W = L + F_B \tag{3.4}$$

For pitching moment equilibrium, the hydrodynamic pitching moment M about the vessel centre of gravity is balanced by the hydrostatic couple of the weight and buoyant force.

A submersible must have its centre of buoyancy B above its centre of gravity G, as indicated in Fig. 3, otherwise it will overturn. If B is directly above G at $\alpha = 0$, then at angle of attack α moment equilibrium requires:

$$M = C_M q A d = \left\{ C_{M_{\alpha=0}} + \frac{dC_M}{d\alpha} \cdot \alpha \right\} q\, Ad = W \cdot \overline{BG} \cdot \alpha \tag{3.5}$$

Therefore:

$$\alpha = \alpha_{Trim} = \frac{C_{M\alpha=0}}{\left(\frac{W}{qA}\,\frac{\overline{BG}}{d}\right) - \frac{dC_M}{d\alpha}} \tag{3.6}$$

W and $\overline{BG}$ are 22,000 lbs and 0.26 ft, respectively (Ref. 3), A = 51.5 sq.ft., $d = \sqrt{A}$ = 7.18 ft., $\frac{dC_M}{d\alpha}$ = +0.020 per degree, and $C_{M_{\alpha=0}}$ is estimated from Fig. 6 to level off at +0.096 for speeds of 1 kt. or more.

On substituting these values in Eq. (3.6), it is found that α_{Trim} rises from +1.3° at V = 1 kt. to +25.2° at V = 2 kts., an impossibly high value, and one reason why Pisces IV could not be operated at speeds much above 1 kt. A record of one test run (Ref. 4) indicates an average speed of 1.18 kts., which would give a q of 3.95 psf. and a value of α_{Trim} = 1.9° from Eq. (3.6). This angle is roughly comparable with the shallow rate of climb the vessel experienced during the test run,

stated to be about 0.09 fps, although no accurate analysis can be made without knowledge of the manner in which the tiltable thrusters were controlled during the run.

3.6 Dynamic Stability in Pitch A more dramatic aspect of Pisces' behaviour in the above test run was a severe oscillation in pitch. The speed did not vary much from the average of 1.18 kts., and the flight path was quite straight, although a shallow climb, as mentioned in the previous section, but the angle of attack α oscillated through a peak-to-peak range of nearly 9°, with an average period θ of 21.6 seconds. This motion is analysed in Appendix A.

By the theory of Appendix A, the pitch oscillation is predicted, and 2 limiting values of the period of oscillation are calculated. With a low estimate of the effective moment of inertia of the submersible and the water moved by it, the period is:

$$\theta_1 = 18 \text{ secs.}$$

With a high estimate of the effective moment of inertia, the period is:

$$\theta_2 = 25 \text{ secs.}$$

The observed average θ of 21.6 secs. lies about midway between the calculated limits. The theory also leads to calculation of a damping factor ζ, the fraction of the amount of system damping that would prevent oscillation altogether. For the same limiting cases of effective moment of inertia, the corresponding damping factors are:

$$\zeta_1 = 0.0097 \qquad \zeta_2 = 0.0068$$

So that the damping is very slight, and would require from 11 to 16 cycles of oscillation (200 to 400 secs.) to reduce an initial angular displacement α_o to half amplitude (Ref. 6).

The analyses of § 3.5 and Appendix A seem to explain satisfactorily the observed behaviour of Pisces IV in the test run of Ref. 4.

4. CHARACTERISTICS OF PISCES WITH FINS

4.1 Preliminary Design Considerations The previous section of the report provides the evidence that the unsatisfactory performance of Pisces IV is caused by its instability to hydrodynamic moments in yaw, and by both its instability to hydrodynamic moments and its low damping in pitch. These problems are solved in naval submarines, aircraft, and dirigibles by providing vertical and horizontal tail fins for stability and control. The fins are either completely moveable about transverse axes, or have moveable trailing-edge portions, and they are frequently located so that they are immersed in the jet, or slipstream, from the thrusting propellers. At least one submersible, Lockheed's 'Deep Quest' (Ref. 7) follows this design philosophy.

Briefly the principles are that the fins develop transverse hydrodynamic forces with long lever arms about the vessel c.g., so that large moments are produced to counter-act the unstable hydrodynamic moments of the basic hull shape, and that these counter-acting forces and moments are magnified for a fin immersed in a high-velocity slipstream.

For Pisces IV, it was decided therefore to introduce a pair of horizontal fins immersed in the slipstreams of the two thrusters, and a pair of vertical fins mounted as far aft on the hull as possible, since they would not be in the slipstreams. Two sets of fins were designed, and tested on the model in the wind tunnel. The larger second set was produced for two reasons; first, because the first set of vertical fins

proved less effective than had been calculated, apparently because of the influence of separated wakes from the sail and the underside of the forward sphere; second, because a more exact calculation of the augmenting effect of the thruster slipstreams on the horizontal fins showed that the effect was less than had originally been estimated, so that larger fins were desirable.

All fins are rectangular in planform, for simplicity of manufacture, and all use the same symmetrical airfoil section shape, the NACA 0015 (Ref. 8, p. 324), which has good aerodynamic characteristics at the moderate Reynolds numbers of Pisces operation. The airfoil shape is given in Fig. 7 and its coordinates are given in percent chord C in an accompanying table. If required additional coordinates can be calculated from the equation under the table.

To provide pitch and yaw control, each pair of horizontal fins and each pair of vertical fins deflects as a rigid unit about a spanwise axis. The planform dimensions and axis locations for all fins are given in Fig. 8. The position of the horizontal fins on the hull is a compromise between a more forward position to obtain the maximum augmentation of lift from the thruster slipstreams, and a further aft position, to give a longer moment arm about the c.g. The shaft connecting the two horizontal fins should be located just forward of the rear pressure sphere, and in the plane of the thrust line of the propellers when they are horizontal (parallel to the deck). It is assumed that the thrusters will no longer be tilted for control. On the model, the shaft of the horizontal fins is located 7.85 inches aft of the c.g. position, or 62.8 inches aft of the c.g. on the actual vessel.

The vertical fins on the model were located so that the trailing edge of the upper fin was at the aft end of the deck. This placed the

vertical shaft 12.0 inches aft of the c.g. on the model, or 96.0 inches aft on the actual vessel. Although a straight connecting shaft was used on the model vertical fins, the rear pressure sphere would interfere with this on the prototype. Separate shafts, connected by a crank, could be used, or the lower fin could be left fixed, and control applied only to the upper fin. The effect of this on lateral control will be considered in § 4.7.

In mounting the fins on the hull, no appreciable gaps between the fin root chord and the hull should be left. Fillets should be added where necessary to ensure this. Modeling clay was used for this purpose in the model tests.

4.2 Pitch Characteristics with Small Fins Figs. 9 and 10 give the pitch and yaw characteristics of the model with the first set of fins mounted, and the thruster nacelles removed. The 3-strut mounting was used for pitch tests, and the 2-strut mounting for yaw tests.

In Fig. 9, curves of C_D, C_L, and C_M are given as functions of α at the usual test R_e, and for $\beta = 0$, and vertical fin deflections $\delta_V = 0$. Five horizontal fin deflections δ_H were tested. There is seen to be little effect of δ_H on C_D, and the drag values are lower than in Fig. 4 for the basic configuration, because of the removal of the nacelles. The curves of C_L show the expected behaviour with δ_H, in that increasing δ_H (downward deflection is positive) raises the C_L curve without changing the slope $\frac{dC_L}{d\alpha}$, which is found to be +0.038 per degree. Thus, the horizontal fins have increased $\frac{dC_L}{d\alpha}$ from +0.025 to +0.038.

For the C_M curves, increasing lift at the stern causes an increase

in bow-down pitching moment (negative), so the C_M curves are lowered by increasing δ_H, again without changing the slope $\frac{dC_M}{d\alpha}$. This is found to be +0.010 per degree, so that the fins have reduced the instability by 50%, from +0.020 per degree. It was estimated originally that the slip-stream augmentation of the fin lift would produce enough additional bow-down C_M to make the vessel stable. This is analysed further in § 4.8.

4.3 Yaw Characteristics with Small Fins Fig. 10 gives curves of C_D, C_S, and C_Y as functions of β for 3 values of δ_V, and for $\alpha = \delta_H = 0$ at the usual R_e. The curves are qualitatively like those of Fig. 9, except that C_S and C_Y are closely antisymmetric functions, because of the symmetry of the model about its vertical centre plane. Here $\frac{dC_S}{d\beta}$ is found to be +0.030 per degree, an increase from +0.025 for the basic vessel shape. Correspondingly, $\frac{dC_Y}{d\beta}$ is +0.011 per degree, still unstable but a reduction from +0.017 per degree for the basic shape. The improvement is much less than had been estimated, apparently because of the adverse effects mentioned in § 4.1. This is analysed further in § 4.7.

4.4 Pitch Characteristics with Large Fins When the first set of fins proved unsatisfactory, the second, larger set shown in Fig. 8 was designed and mounted, and Figs. 11, 12, and 13 give the characteristics in pitch, in yaw, and with Reynolds number. In Fig. 11, the pitch results are presented as in Fig. 9, except that only 3 values of δ_H were tested, and α could not be taken below -5°, because the tall vertical fin would otherwise come too close to the tunnel ceiling.

The curves are qualitatively like those of Fig. 9, but now the larger

fins have caused an increase in $\frac{dC_L}{d\alpha}$ to +0.052 per degree, and a corresponding decrease in $\frac{dC_M}{d\alpha}$ to +0.001 per degree, so that the instability has been nearly eliminated even without the augmentation of the slip-stream. Furthermore, the amount of pitch control is considerably increased, as measured by the change in C_M with δ_H. This is shown in Fig. 14, from which the slope of the curve $\frac{dC_M}{d\delta_H}$ is seen to be increased from -0.010 per degree for the small fins to -0.017 per degree for the large fins.

4.5 Yaw Characteristics with Large Fins In Fig. 12, the yaw results are presented as in Fig. 10. The tall upper vertical fin behaves more like a conventional aircraft wing of large span than the other fins tested, and it shows an appreciable drag increase and eventual stall as its angle to the approaching air flow, $\beta + \delta_V$, reaches large positive or negative values. The dotted portions of the curves indicate ranges where this fin is near the stall.

Otherwise, it is seen that the larger upper fin has caused $\frac{dC_S}{d\beta}$ to increase to +0.041 per degree, while $\frac{dC_Y}{d\beta}$ has been reduced to -0.002 per degree, so that the vessel is now slightly stable in yaw. Also, the yaw control has been greatly increased, as measured by the change of C_Y with δ_V. This is shown in Fig. 14, from which $\frac{dC_Y}{d\delta_V}$ is seen to be increased from -0.007 per degree for the small fins to -0.016 per degree for the large fins.

4.6 Reynolds Number Characteristics with Large Fins The effects of R_e on the basic Pisces configuration at $\alpha = 0, \beta = 0$ were presented in Fig. 6 and discussed in §3.3. Similar tests were carried out for the model with large fins mounted, and the results are presented in Fig. 13.

Again C_D and C_M are seen to decrease with increasing R_e, and again the decrease is quite small from the test R_e of $0.61(10)^6$ to the beginning of the relevant full-scale range at $R_e = 0.76(10)^6$, about 2% for C_D and 6% for C_M.

The causes of the increase in C_L with R_e shown are not clear. One cause of a spurious effect may be a deflection of the model to increasingly positive α under the increasing dynamic pressure. In any case the values of C_L are quite small, and would correspond to only about 14 lbs lift on the actual vessel at a speed of 1 knot.

4.7 Analysis of the Fin Characteristics The performance of the fins as measured in the wind tunnel can be compared with the predictions of aerodynamic theory by considering $\frac{dC_L}{d\alpha}$, $\frac{dC_M}{d\alpha}$, $\frac{dC_S}{d\beta}$, and $\frac{dC_Y}{d\beta}$ for the model with and without fins, and using the data to determine the effective lift curve slope of each of the fins $\frac{dC_F}{d\alpha}$ or $\frac{dC_F}{d\beta}$, where C_F, as defined in the Nomenclature, is the force on the fin normal to the span and to the approaching flow, whether the fin is horizontal or vertical.

The method of determining $\frac{dC_F}{d\alpha}$ or $\frac{dC_F}{d\beta}$ is described in Appendix B and the results are as follows, with 2 values shown for each fin, one calculated from the force data and the other calculated independently from the moment data:

Small horizontal fins: $\frac{dC_F}{d\alpha} = .058, .060$

Large horizontal fins: $\frac{dC_F}{d\alpha} = .060, .057$

Small vertical fins: $\frac{dC_F}{d\beta} = .022, .024$

Large vertical fins: $\frac{dC_F}{d\beta} = .048, .050$

The close agreement in each case of the 2 independent values tends to confirm their accuracy. Several inferences can be drawn from the results. It is seen that $\frac{dC_F}{d\alpha}$ is about the same for both sets of horizontal fins, with an average value (to 2 significant figures) of .059. This is not surprising, since both sets have the same square planform as well as the same airfoil section. Aerodynamic theory (Ref. 8, p. 11) for a wing made up of two square fins as half-wings would predict $\frac{dC_F}{d\alpha} = .044$, so the hull between the two fins is carrying some of the lift they create. This is to be expected, and is counted on in aeronautical practice.

Although the small vertical fins are identical with the small horizontal fins, they achieve only 40% of their performance. This must be because of the reduced-velocity wakes of the sail and the underside of the forward pressure sphere flowing over the vertical fins. When the taller upper vertical fin is introduced, the value of $\frac{dC_F}{d\beta}$ is more than doubled, although the fin area has been increased by only 50%, because the added portion is clear of the wake of the sail. If the incremental lift of the added upper portion is calculated as a coefficient C_F' based on the added area, then

$$\frac{dC_F'}{d\beta} = 3(.049) - 2(.023) = .101 \text{ per degree}$$

about the right value for the airfoil section used.

The above estimates of the fin performance are also compatible with the observed control characteristics of Fig. 14, although values of $\frac{dC_F}{d\delta_H}$ for the large horizontal fins would be somewhat lower than $\frac{dC_F}{d\alpha}$ values, because of the root gaps that open up as the fins are deflected. For the vertical fins, the above results indicate that if the lower fin was fixed, and only the enlarged upper fin deflected for control, the

reduction in control as measured by $\frac{dC_Y}{d\delta_V}$ would be quite small, from -0.016 to -0.013 per degree.

4.8 Slipstream Augmentation of Horizontal Fin Performance A simple and plausible method of estimating the augmentation of fin lift caused by immersion in a slipstream would be to increase the lift on that portion of the fin immersed in the slipstream in proportion to the increase in dynamic pressure $(q_j - q)$, where q_j is the jet dynamic pressure. This method was used for the preliminary design calculations for the first set of horizontal fins.

However, subsequent study of a report on some recent research on wing-slipstream interaction (Ref. 9) revealed that the above method greatly overestimates the augmentation, and that another relatively simple theory, proposed some years ago (Ref. 10) in fact gives quite accurate estimates of slipstream augmentation.

According to this theory, the increment in lift on one fin is given by:

$$\Delta L = .1096\alpha (q_j - q)\, d_j^2 \left\{ \frac{1}{4} - \frac{T_c}{2\pi^2} \right\} \qquad (4.1)$$

where $T_c = \frac{1}{(q_j/q + 1)} \frac{4C_D A}{\pi d_j^2}$

d_j = jet diameter

When this increment is converted to coefficient form, and calculated for Pisces IV with the large fins, the resulting increment in $\frac{dC_M}{d\alpha}$ is

$$\Delta \frac{dC_M}{d\alpha} = -0.0039 \text{ per degree}$$

Therefore, the resulting value is

$$\frac{dC_M}{d\alpha} = +0.001 - 0.004 = -0.003 \text{ per degree}$$

and the vessel is now stable in pitch with respect to hydrodynamic moments.

Also, when the pitch damping is calculated for the large fins by the method of Appendix B, and the effect of the changed $\frac{dC_M}{d\alpha}$ is included, the oscillatory behaviour changes so that the calculated limiting cases are now

$$\theta_1 = 15 \text{ secs.}, \zeta_1 = 0.19$$

and

$$\theta_2 = 21 \text{ secs.}, \zeta_2 = 0.14$$

The damping is now very effective, and would require less than 1 cycle of oscillation (9 to 16 secs) to reduce an initial angular displacement α_o to half amplitude.

The augmentation of Eq. (4.1) would increase the pitch control, as measured by $\frac{dC_M}{d\delta_H}$, from -0.017 to -0.020 per degree.

5. RECOMMENDATIONS AND DISCUSSION

5.1 Recommended Modifications of Pisces IV The submersible should be fitted with the larger fins as described in §4.1, illustrated in Figs. 1 and 2, and detailed in Figs. 7 and 8. The horizontal fins should be mounted on a common shaft as described in §4.1. The vertical fins should have only the tall upper fin controllable, for simplicity. The thrusters should be fixed in position with their thrust line parallel to the deck and the horizontal fins should lie in the plane of the thrust line.

5.2 Fin Hinge Moments The design of the pilot's controls requires a knowledge of the hydrodynamic moments at the fin axes. For the horizontal fins, the lift force, including augmentation, can be assumed to act 1.2 inches behind the axis, and to correspond to a maximum lift coefficient C_F of 1.0. With a total horizontal fin area A_F of 23.1 sq. ft., and a dynamic pressure q of 11.44 psf at 2 kts., the maximum horizontal fin hinge moment

H_H will be

$$H_H = 1.0(11.44)23.1(1.2) = 318 \text{ lb-in.}$$

at 3 kts., $H_H = (\frac{3}{2})^2\ 318 = 715$ lb-in.

For the upper vertical fin, the force can again be assumed to act 1.2 inches behind the axis, and to correspond to a maximum force coefficient C_F of 1.0. With a fin area of 11.5 sq. ft., and a q of 11.44 psf at 2 kts, the vertical fin hinge moment H_V will be

$$H_V = 1.0\ (11.44)11.5(1.2) = 158 \text{ lb-in.}$$

At 3 kts. $H_V = (\frac{3}{2})^2 158 = 355$ lb-in.

5.3 New Trim Conditions The large fins ensure the stability of the submersible in pitch and yaw. The horizontal fins also correct the impossible trim requirements of the basic configuration. Taking the new values of $C_{M_{\alpha=0}}$ and $\frac{dC_M}{d\alpha}$ to be +0.10 (Fig. 13) and -0.003 (§ 4.8) respectively, new values of α_{Trim} are calculated from Eq. (3.6):

V = 1 kt. $\alpha_{Trim} = 1.0°$

V = 2 kts. $\alpha_{Trim} = 3.7°$

V = 3 kts. $\alpha_{Trim} = 7.4°$

These trim conditions are for the case where B is directly above G when the deck is horizontal. The submersible can be trimmed at $\alpha = 0$ at any of the above speeds merely by shifting G forward the appropriate distance for that speed.

5.4 Final Remarks This report provides the hydrodynamic analysis and design for the modifications needed to make the performance of the Pisces IV satisfactory for her presente role. It is assumed that the detailed mechanical design will be carried out by engineers of the

Marine Sciences Directorate.

The degree of pitch and yaw stability achieved by adding the large fins is moderate, but should be adequate. The pitch stability to hydrodynamic moments may actually prove larger than estimated, because there is some experimental evidence that effects of slipstream augmentation on fin lift will be larger than calculated by Eq. (4.1). The yaw stability might be increased by reducing the wakes of the sail and forward sphere that impinge on the vertical fins, through improved streamlining, and the yaw control can, if necessary, be supplemented by differential thrust control, but it should be realized that this will now introduce a rolling moment on the submersible, since the horizontal fin immersed in the higher-thrust slipstream will develop more lift than the other one.

REFERENCES

1. J. R. McFarlane, 'Pisces Class Model Tests in the UBC Wind Tunnel', Internal HYCO Report, July, 1971.
2. A. M. Riddell, 'The Theory and Practice of the Kort Nozzle System of Propulsion', Trans. INA, 1942, pp. 87-114.
3. S. Lee, 'Stability Test, Pisces IV',Internal HYCO Report, April, 1972.
4. (Rough Data Sheets, Author Unidentified) 'Initial Stability Measurements of Pisces IV', November 14, 1973.
5. H. Lamb 'Hydrodynamics', Dover, 1945, p. 155.
6. W.T. Thomson 'Mechanical Vibrations', Prentice-Hall, 1953, p. 57.
7. E.H. Shenton 'Diving for Science', Norton, 1972, p. 210.
8. I.H. Abbott and A.E. von Doenhoff, 'Theory of Wing Sections', Dover, 1959.
9. N.D. Ellis, 'Aerodynamics of Wing-Slipstream Interaction. A Numerical Study' UTIAS Report 169, October, 1971.
10. E.W. Graham, P.A. Lagerstrom, R.M. Licher, B.J. Beane, ' A Preliminary Theoretical Investigation of the Effects of Propeller Slipstream on Wing Lift', Douglas Aircraft Report SM-14991, 1953.

APPENDIX A

ANALYSIS OF PITCHING OSCILLATIONS

For a rigid vessel, moving in its vertical plane of symmetry, there are 3 equations of motion, one each for horizontal, vertical and pitching motions. However, the evidence of nearly constant speed and a nearly straight flight path indicates that horizontal and vertical accelerations are small, so it will be assumed that horizontal and vertical forces are respectively in equilibrium, and only the pitching equation of motion need be considered. With the vessel experiencing an angular acceleration $\ddot{\alpha} = \frac{d^2\alpha}{dt^2}$, equilibrium Eq. (3.5) is replaced by

$$(J + K'J')\ddot{\alpha} = -W\overline{BG}\,\alpha + M \qquad (A.1)$$

where J = polar moment of inertia of submersible about c.g.

J' = polar moment of inertia of displaced volume of submersible about c.g.

K' = apparent mass moment of inertia coefficient

and M now depends on both α and angular velocity $\dot{\alpha} = \frac{d\alpha}{dt}$:

$$M = \frac{\partial M}{\partial \alpha}\alpha + \frac{\partial M}{\partial \dot{\alpha}}\dot{\alpha}$$

Thus, Eq. (A.1) can be written in the form:

$$j\ddot{\alpha} + r\dot{\alpha} + k\alpha = 0 \qquad (A.2)$$

where $j = J + K'J'$

$$r = -\frac{\partial M}{\partial \dot{\alpha}}$$

$$k = W\,\overline{BG} - \frac{\partial M}{\partial \alpha}$$

Eq. (A.2) has the solution

$$\alpha = \alpha_o e^{-\frac{rt}{2j}} \cos\sqrt{\frac{k}{j} - \left(\frac{r}{2j}\right)^2}\, t \qquad (A.3)$$

if $r^2 < 4jk$

The torsional spring constant k is known from § 3.5, but effective moment of inertia j and damping constant r must be estimated for Pisces IV in order to relate Eq. (A.3) to the observed behaviour. The moment of inertia J of the submersible was not available, but it can be estimated roughly by assuming all of the weight to be in the two steel spheres. This gives J = 22,500 slug-ft^2, corresponding to a radius of gyration of 5.74 ft.

The moment of inertia J' of the displaced volume is calculated by two methods. For a lower limit, the hull shape is assumed to be a prolate ellipsoid of about the same dimensions as the actual hull. This gives J' = 23,100 slug-ft^2, and the corresponding value of coefficient K' = 0.45 (Ref. 5). For an upper limit, the hull shape is assumed to be a circular cylinder of appropriate dimensions, giving J' = 54,300 slug-ft^2, and the corresponding value of K' = 0.80.

The pitch damping constant r is difficult to estimate for the basic configuration of the submersible. However, when horizontal fins are added, most of the damping comes from them, and can be calculated easily. This is done in Appendix B, for the final set of fins used, and r is calculated to be 4500 lb-ft-sec without slipstream augmentation, or 5400 lb-ft-sec with augmentation at 1.18 kts. In aeronautical practice, it is common to add 10% to the calculated pitch damping of the tail to allow for the effect of the wing and fuselage. Here it seems reasonable, therefore, to take the value of r for the basic configuration (corresponding to a rather short fuselage) as 5% of the value without augmentation calculated above, or 225 lb-ft-sec. Also,

$$\frac{\partial M}{\partial \alpha} = \frac{dC_M}{d\alpha} \; qAd = +0.020(3.95)51.5(7.18)$$

$$= +29.4 \text{ lb-ft per degree}$$

$$= 1700 \text{ lb-ft per radian}$$

Therefore, k = 22,000(.26)-1700 = 4000 lb-ft per radian. As estimated above, r = 225 lb-ft-sec. The two estimates of K'J' lead to

$$j_1 = 22{,}500 + 0.45(23{,}100) = 33{,}000 \text{ slug-ft}^2$$

$$j_2 = 22{,}500 + 0.80(54{,}300) = 66{,}000 \text{ slug-ft}^2$$

The true effective j should lie between these values. Examination of the size of terms shows that

$$\left(\frac{r}{2j}\right)^2 << \frac{k}{j}$$

So that Eq.(A.3) holds, and can be simplified to

$$\alpha = \alpha_0 e^{-\zeta\omega t}\cos\omega t \qquad (A.4)$$

where

$\zeta = \frac{r}{2j\omega}$ fraction of critical damping.

$\omega = \sqrt{k/j}$ undamped natural frequency.

Here, $\omega_1 = \sqrt{\frac{4000}{33{,}000}} = 0.35$ rad/sec.

Period $\theta_1 = \frac{2\pi}{\omega_1} = \frac{2\pi}{0.35} = \underline{18}$ secs.

And $\omega_2 = \sqrt{\frac{4000}{66{,}000}} = 0.25$ rad/sec.

$$\theta_2 = \frac{2\pi}{0.25} = \underline{25} \text{ secs.}$$

Also,

$$\zeta_1 = \frac{225}{2(33{,}000)0.35} = \underline{0.0097}$$

$$\zeta_2 = \frac{225}{2(66{,}000)0.25} = \underline{0.0068}$$

APPENDIX B

FIN CHARACTERISTICS

B.1 Determining Fin Performance from Overall Submersible Data The differences in lift and pitching moment for the model with and without horizontal fins are assumed to give independent estimates of the horizontal fin lift curve slope $\frac{dC_F}{d\alpha}$ by the relations:

$$C_{L_{\text{Fins On}}} - C_{L_{\text{Fins off}}} = C_F$$

or

$$\left(\frac{dC_L}{d\alpha}\right)_{\text{Fins On}} - \left(\frac{dC_L}{d\alpha}\right)_{\text{Fins Off}} = \left(\frac{A_F}{A}\right) \frac{dC_F}{d\alpha} \tag{B.1}$$

and

$$C_{M_{\text{Fins On}}} - C_{M_{\text{Fins Off}}} = C_F \ell$$

or

$$\left(\frac{dC_M}{d\alpha}\right)_{\text{Fins On}} - \left(\frac{dC_M}{d\alpha}\right)_{\text{Fins Off}} = \left(\frac{A_F}{A}\right) \left(\frac{\ell}{d}\right) \frac{dC_F}{d\alpha} \tag{B.2}$$

Similarly, the differences in side force and yawing moment for the model with and without vertical fins are assumed to give independent estimates of the vertical fin lift curve slope $\frac{dC_F}{d\beta}$ by the relations:

$$C_{S_{\text{Fins On}}} - C_{S_{\text{Fins Off}}} = C_F$$

or

$$\left(\frac{dC_S}{d\beta}\right)_{\text{Fins On}} - \left(\frac{dC_S}{d\beta}\right)_{\text{Fins Off}} = \left(\frac{A_F}{A}\right) \frac{dC_F}{d\beta} \tag{B.3}$$

and

$$Y_{\text{Fins On}} - Y_{\text{Fins Off}} = F\ell$$

or

$$\left(\frac{dC_Y}{d\beta}\right)_{\text{Fins On}} - \left(\frac{dC_Y}{d\beta}\right)_{\text{Fins Off}} = \left(\frac{A_F}{A}\right) \left(\frac{\ell}{d}\right) \frac{dC_F}{d\beta} \tag{B.4}$$

Values of $\frac{dC_F}{d\alpha}$ and $\frac{dC_F}{d\beta}$ determined in this way include any effects of variations of the flow approaching the fins from the uniform flow at velocity V on which the coefficients are defined.

B.2 Determining Pitch Damping of Horizontal Fins

When the submersible is rotating bow up at angular velocity $\dot{\alpha}^\circ$ (Fig. 15), the horizontal fin is moving down at velocity $\ell\dot{\alpha}^\circ$, so the flow relative to the fin appears to be approaching it at angle of attack

$$\arctan \frac{\ell\dot{\alpha}^\circ}{V} \doteq \frac{\ell\dot{\alpha}^\circ}{V}$$

since $\ell\dot{\alpha}^\circ \ll V$

Therefore, the fin develops a quasi-steady component of lift due to the pitch angular velocity,

$$F_{\dot{\alpha}} = \frac{dC_F}{d\alpha} \left(\frac{\ell\dot{\alpha}^\circ}{V}\right) qA_F$$

and a corresponding component of pitching moment

$$M_{\dot{\alpha}} = -F_{\dot{\alpha}} \cdot \ell = \frac{+\partial M}{\partial \dot{\alpha}^\circ} \dot{\alpha}^\circ$$

Therefore

$$\frac{\partial M}{\partial \dot{\alpha}^\circ} = \frac{-dC_F}{d\alpha} \frac{q}{V} \ell^2 A_F \qquad \text{(B.5)}$$

For the test run at V = 1.18 kts., q = 3.95 psf, assume that the large horizontal fins of A_F = 23.1 sq. ft., with ℓ = 5.33 ft., had been fitted. Then, with

$$\frac{dC_F}{d\alpha} = .059 \text{ per degree} = 3.4 \text{ per radian}$$

without augmentation, and

$$= .071 \text{ per degree} = 4.1 \text{ per radian}$$

with augmentation, substitution in Eq. (B.5) gives

$$r = \frac{-\partial M}{\partial \dot{\alpha}^\circ} = 4500 \text{ lb-ft-sec.}$$

without augmentation, and

$$= 5400 \text{ lb-ft-sec.}$$

with augmentation. Also, for this case

$$\frac{\partial M}{\partial \alpha} = -250 \text{ lb-ft. per radian}$$

so that the two extremes of moment of inertia now correspond to periods of oscillation θ and damping factors ζ, calculated by the methods of Appendix A:

$$\theta_1 = 15 \text{ secs}, \quad \zeta_1 = 0.19$$

and

$$\theta_2 = 21 \text{ secs}, \quad \zeta_2 = 0.14$$

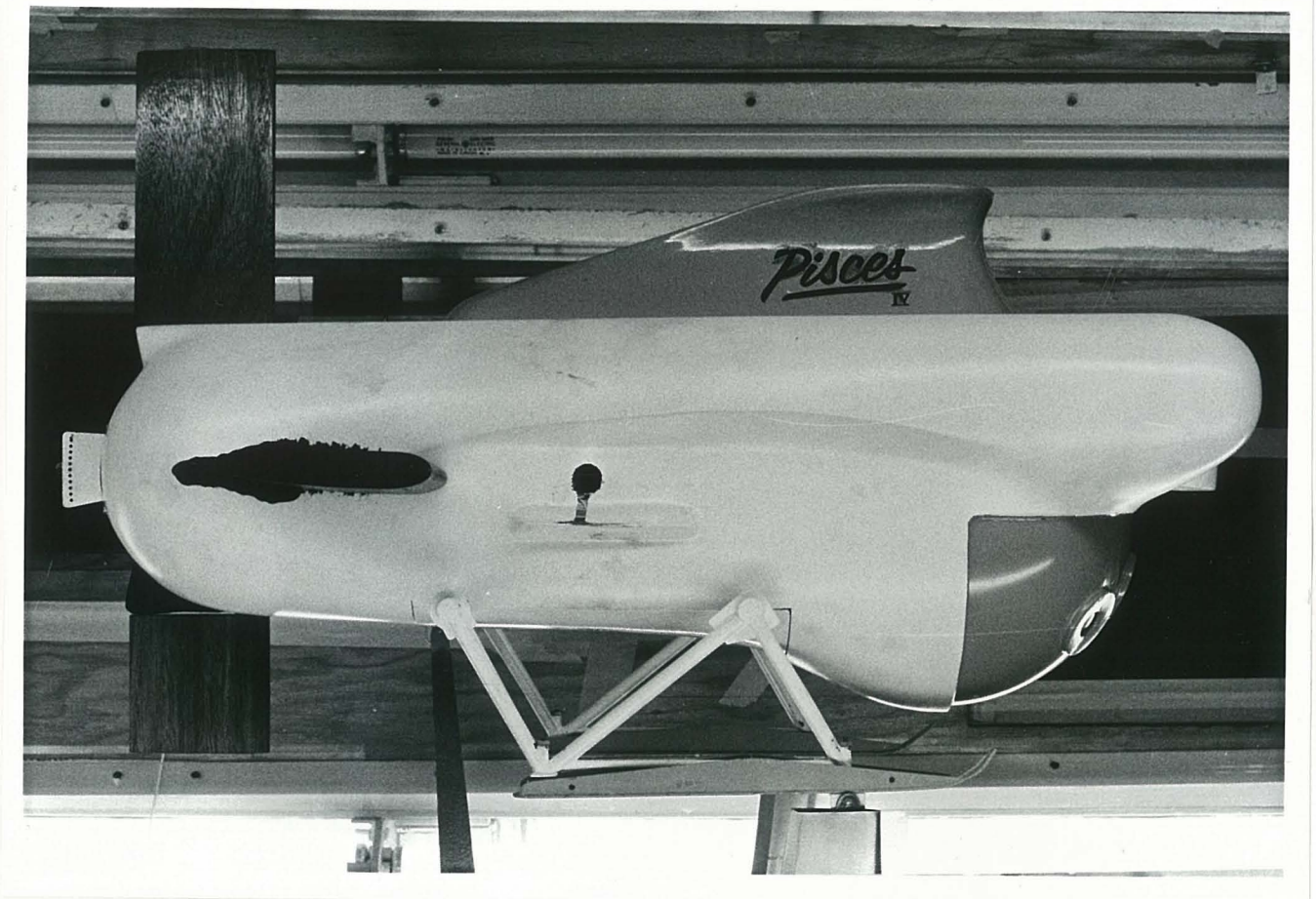

Figure 1 - Side Elevation of Pisces IV Model in Wind Tunnel on 3-Strut Mounting. Large Fins On. Thruster Nacelles Off.

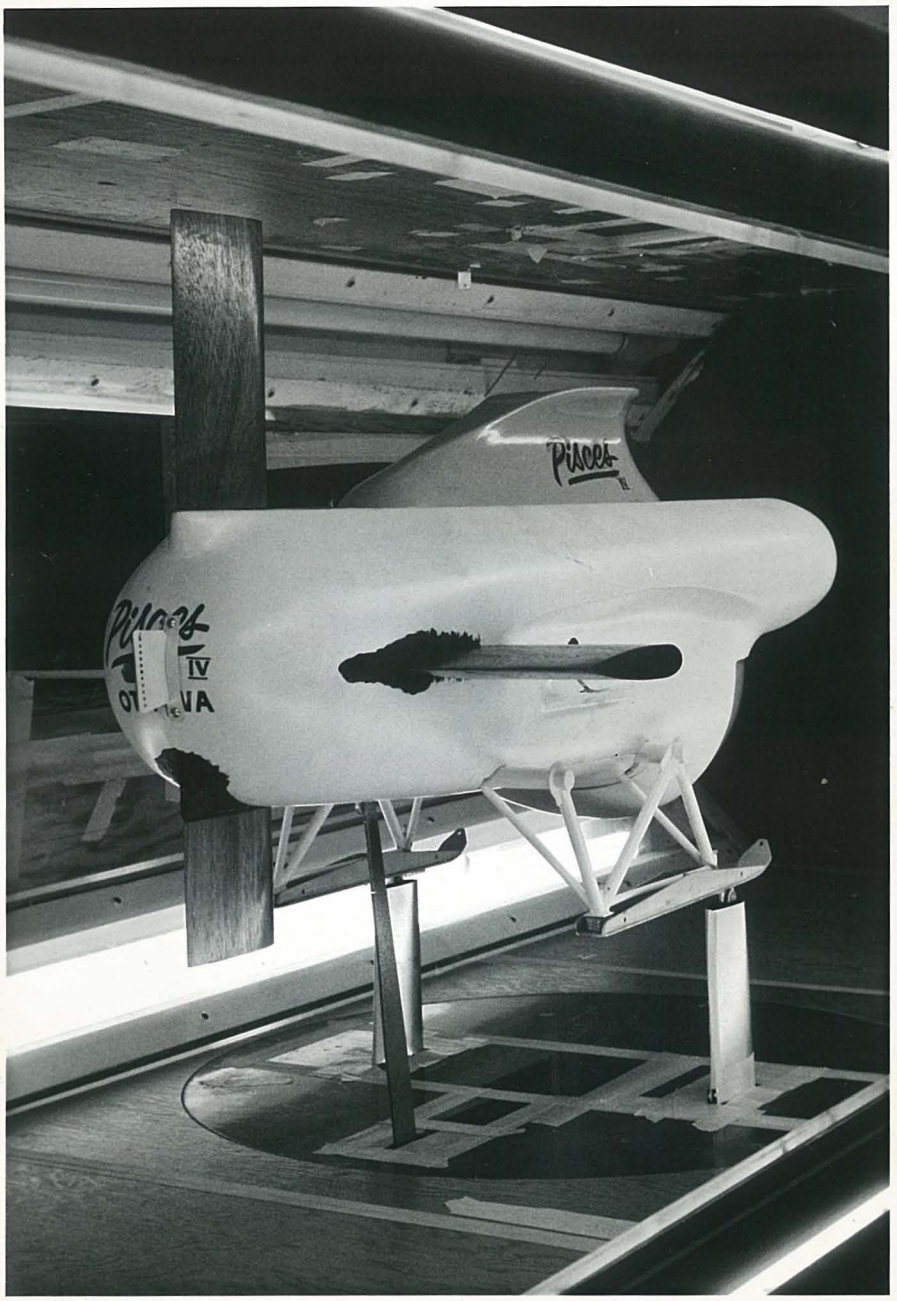

Figure 2 - Three-Quarter Rear View of Pisces IV Model in Wind Tunnel on 3-Strut Mounting. Large Fins On. Thruster Nacelles Off.

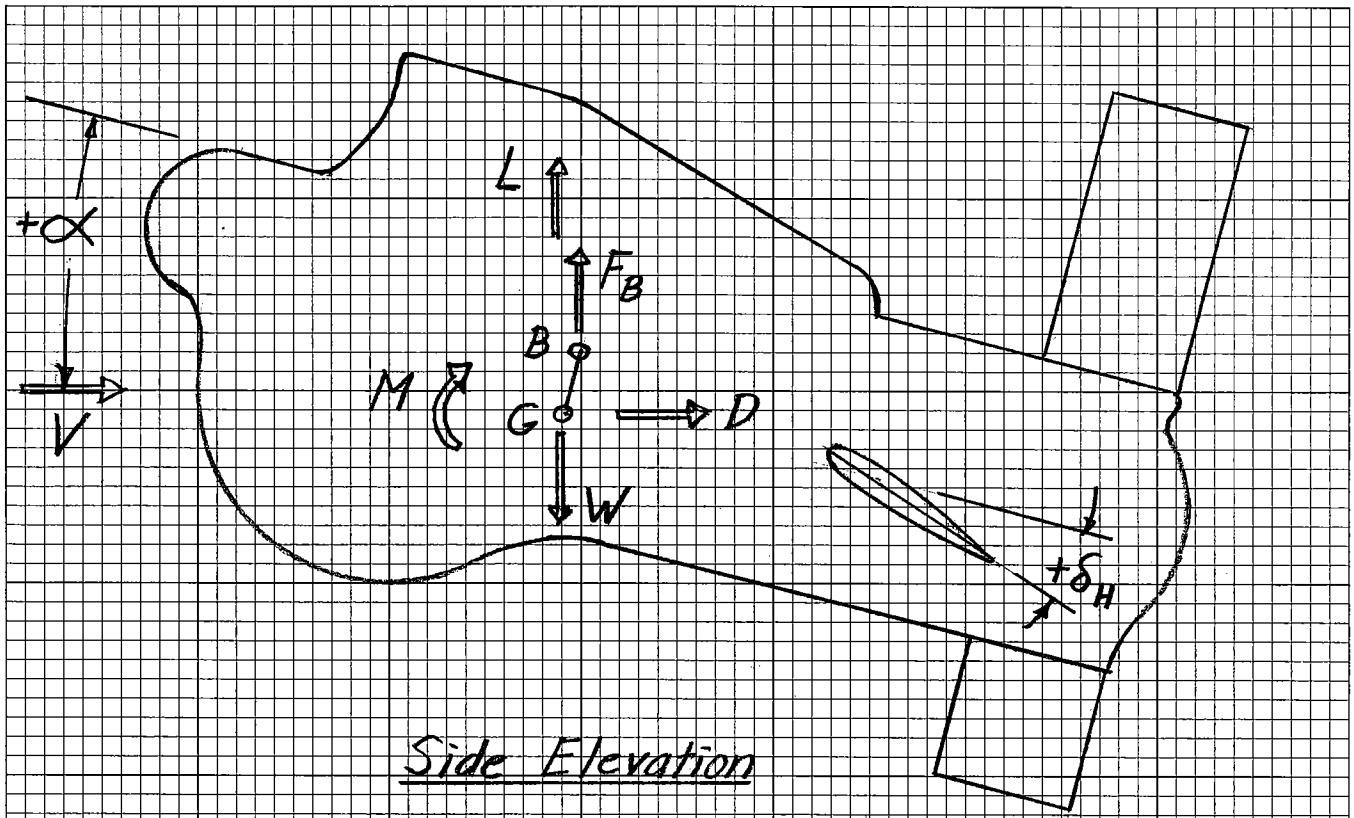

Side Elevation

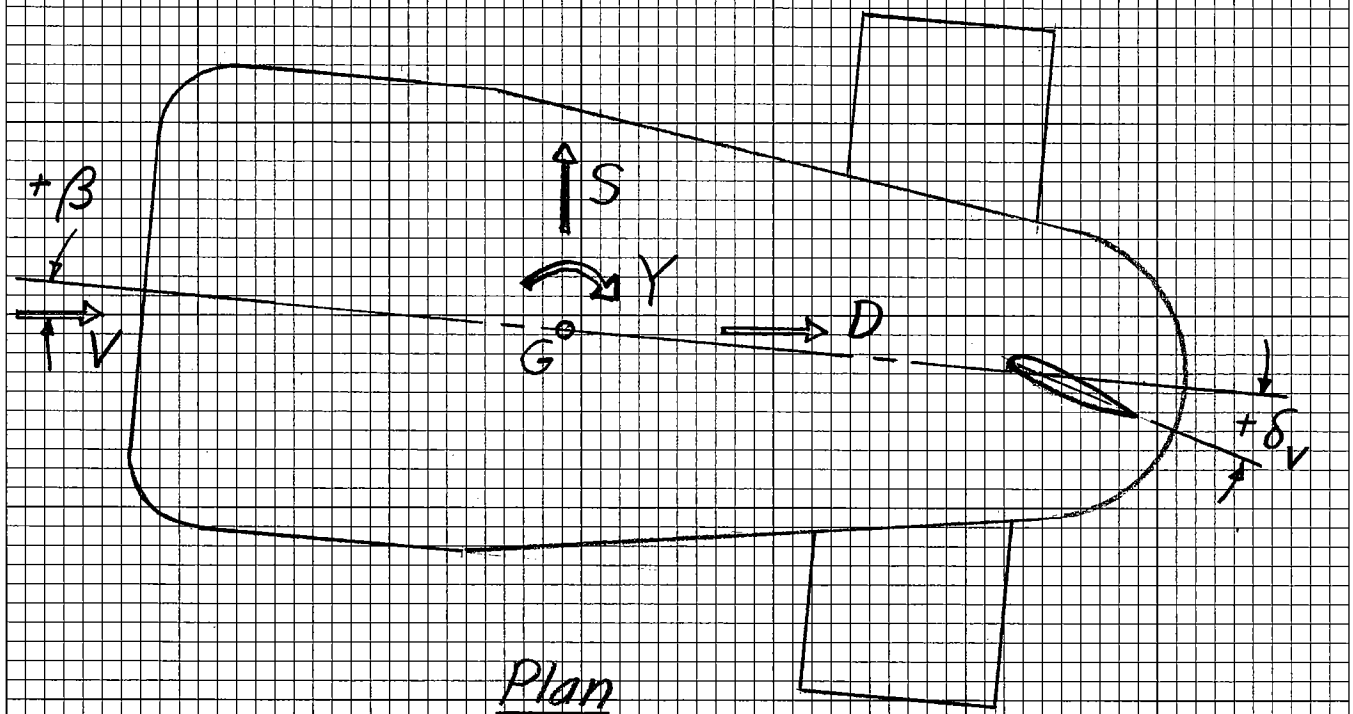

Plan

Figure 3 - Definition of Aerodynamic and Hydrodynamic Terms

Figure 4 - Characteristics in Pitch

Pisces IV - Basic Configuration

$\beta = 0°$, $R_e = 5.9 (10)^5$, Nacelles On

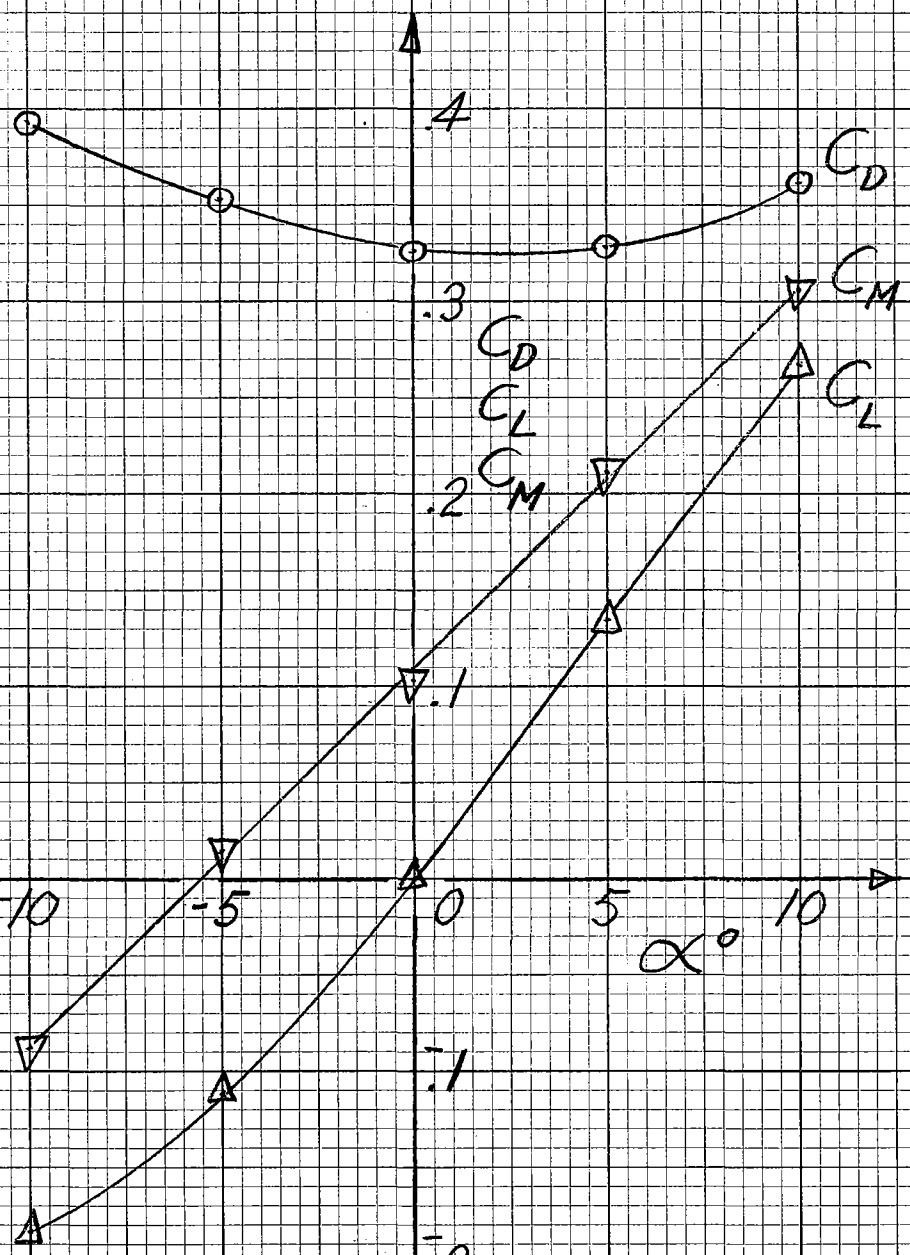

Figure 5 - Characteristics in Yaw
Pisces IV - Basic Configuration

$\alpha = 0^\circ$ $R_e = 5.9(10)^5$ Nacelles On

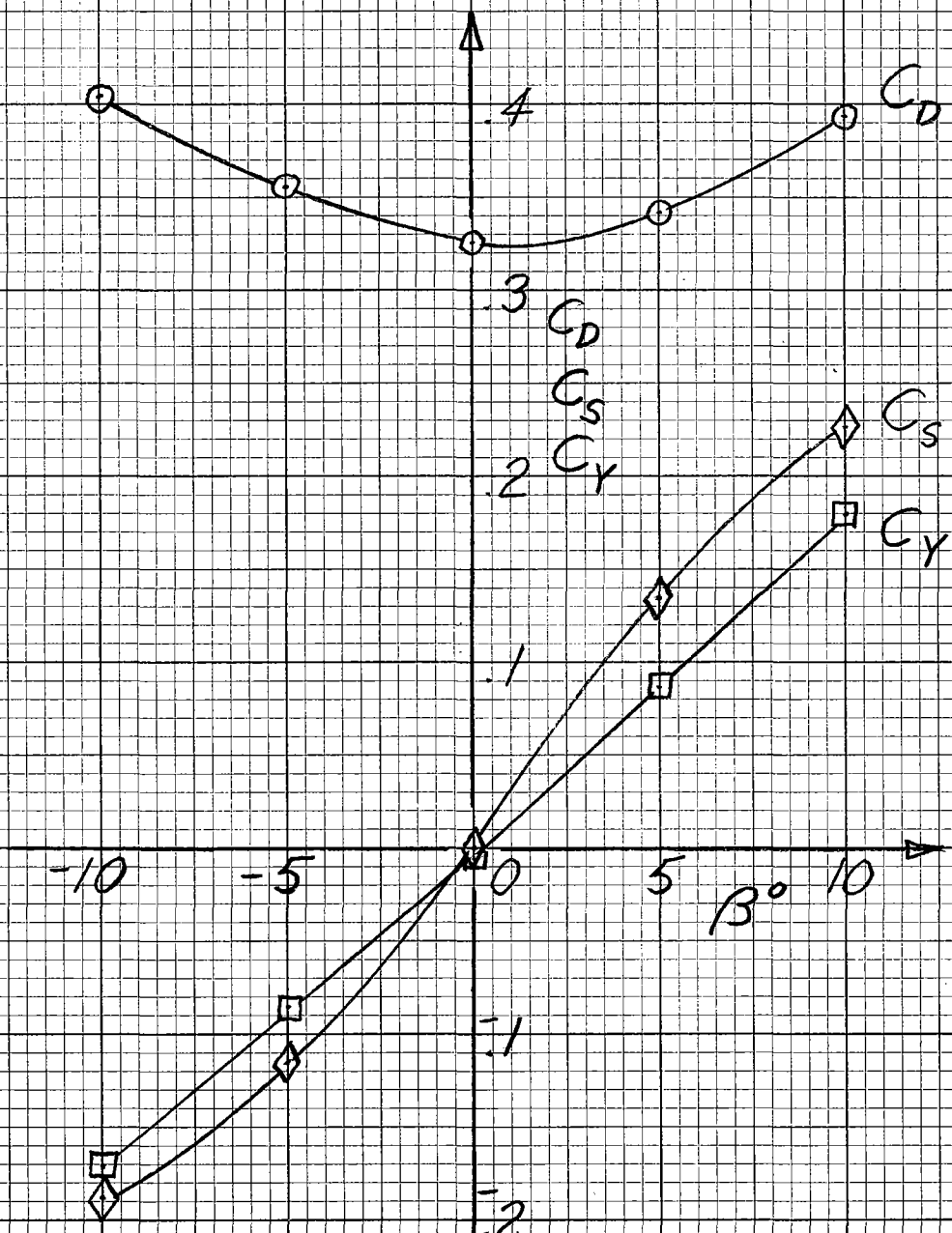

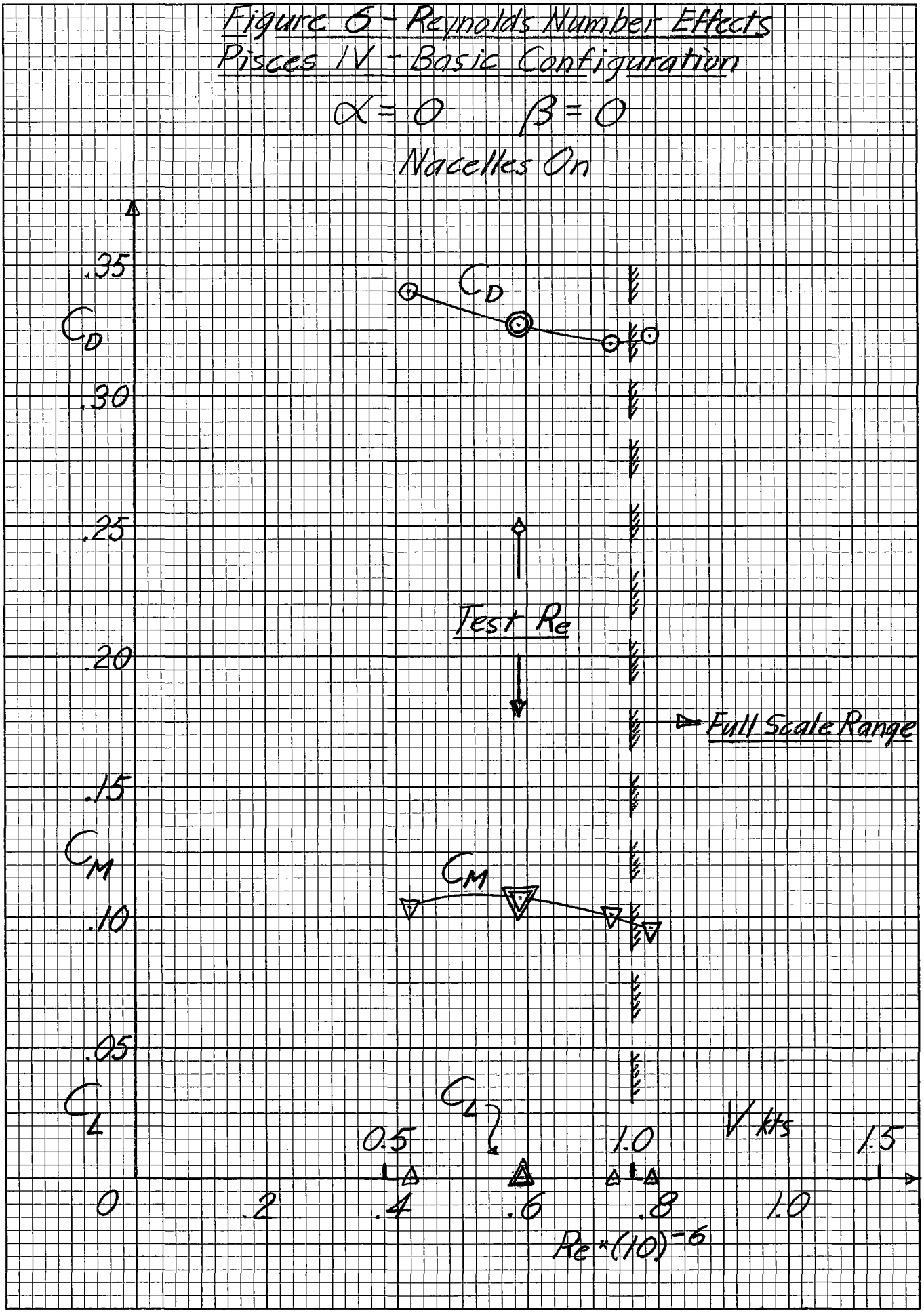
Figure 6 - Reynolds Number Effects
Pisces IV - Basic Configuration
α = 0 β = 0
Nacelles On
.35
C_D
.30
.25
.20
.15
C_M
.10
.05
C_L
0
C_D
Test Re
Full Scale Range
C_M
C_L
0.5
1.0
1.5
V kts
.2
.4
.6
.8
1.0
Re*(10)$^{-6}$

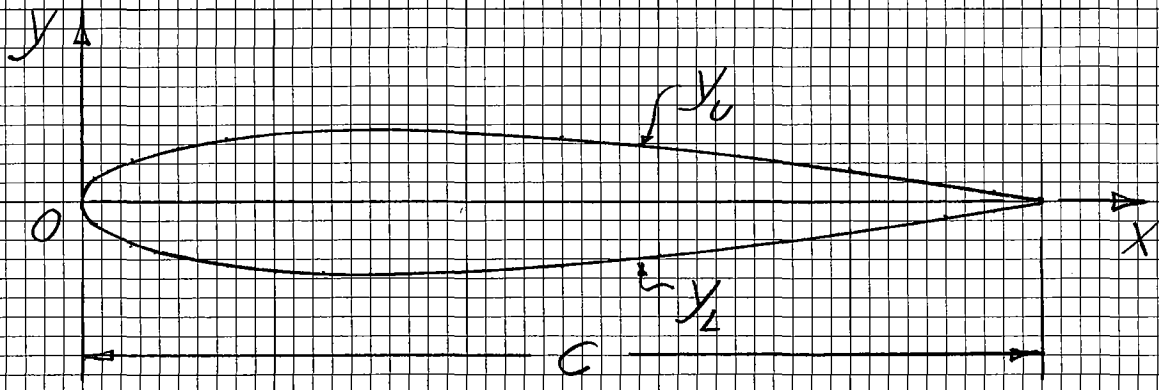

Leading Edge Radius 2.48 %C

X and y in percent C

X	0	1.25	2.5	5.0	7.5	10
$y_u, -y_L$	0	2.367	3.268	4443	5.250	5.853
X	15	20	25	30	40	50
$y_u, -y_L$	6.682	7.172	7.427	7.502	7.254	6.617
X	60	70	80	90	95	100
$y_u, -y_L$	5.704	4.580	3.279	1.810	1.008	0.158

$$y_{u,L} = \pm \frac{3}{4}\left\{.2969\sqrt{X} - .1260X - .3516X^2 + .2843X^3 - .1015X^4\right\}$$

In the equation, X and y are in fractions of C

Figure 7 - NACA 0015 Airfoil Section

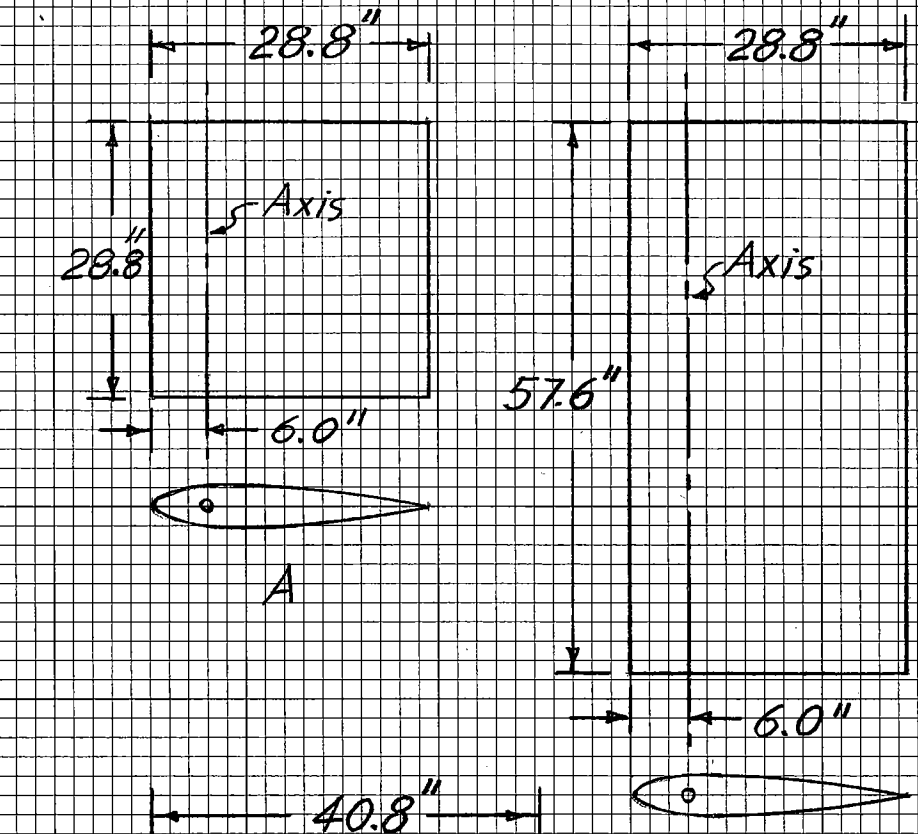

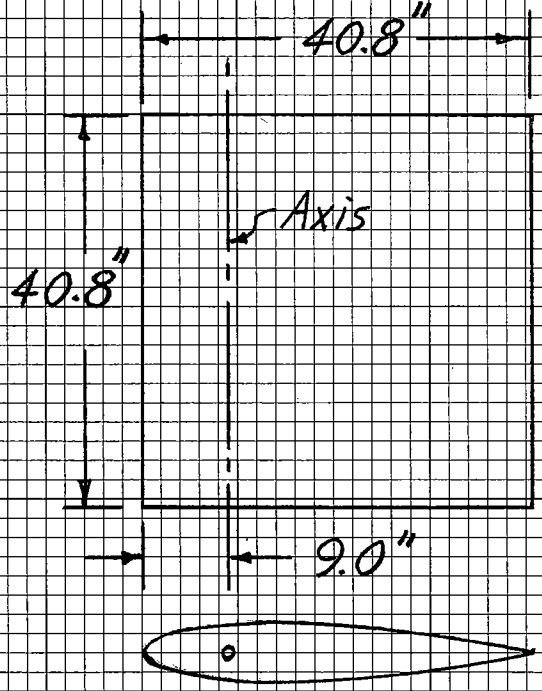

A : All fins of small set. Lower vertical fin of large set.

B : Upper vertical fin of large set.

C : Horizontal fins of large set.

All fins use NACA 0015 Airfoil section

Figure 8 - Details of Horizontal and Vertical Fins

Figure 9 - Pisces IV Pitch Characteristics. Small Fins On. Nacelles Off

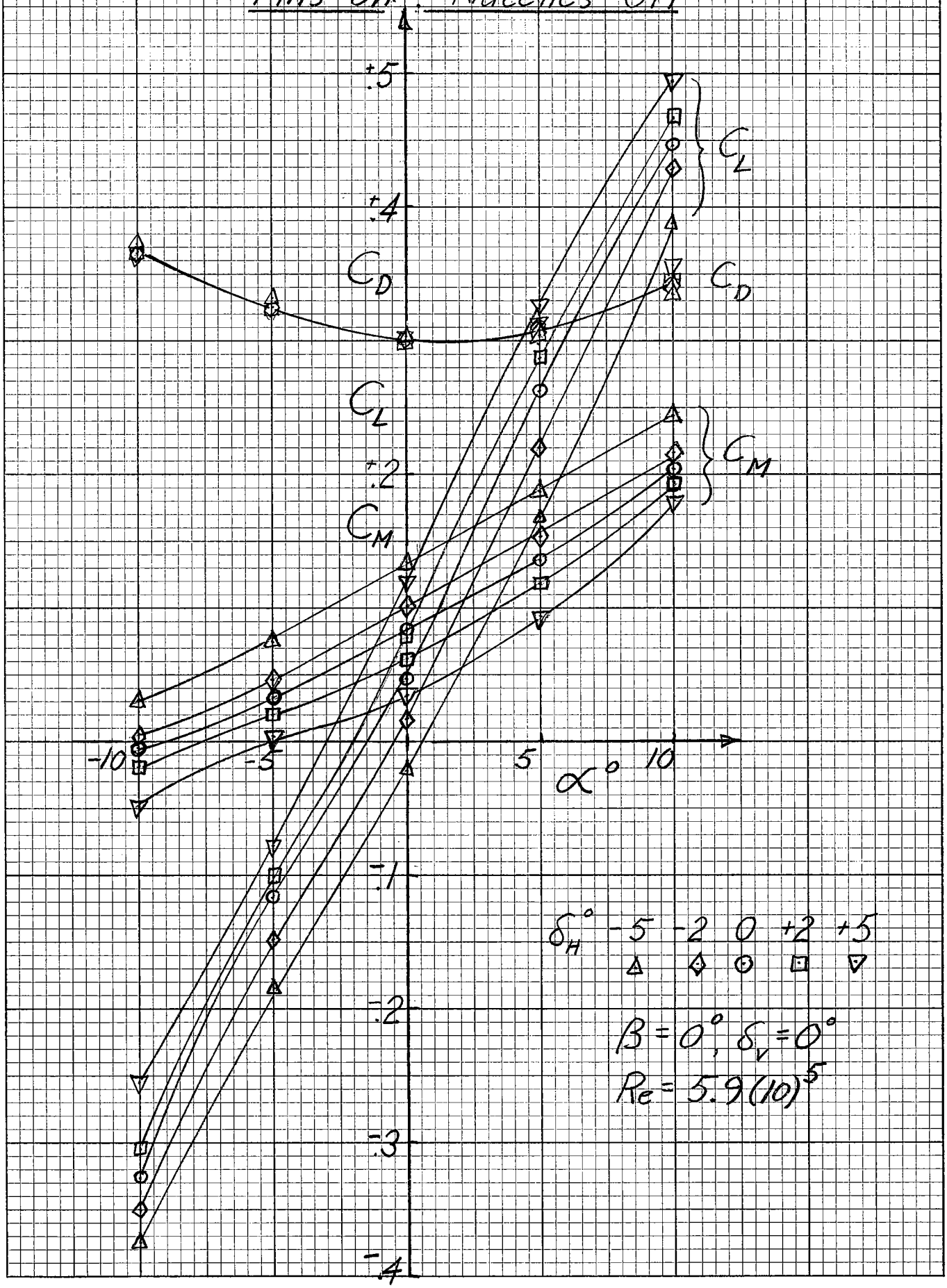

Figure 10 - Pisces IV Yaw Characteristics
Small Fins On. Nacelles Off

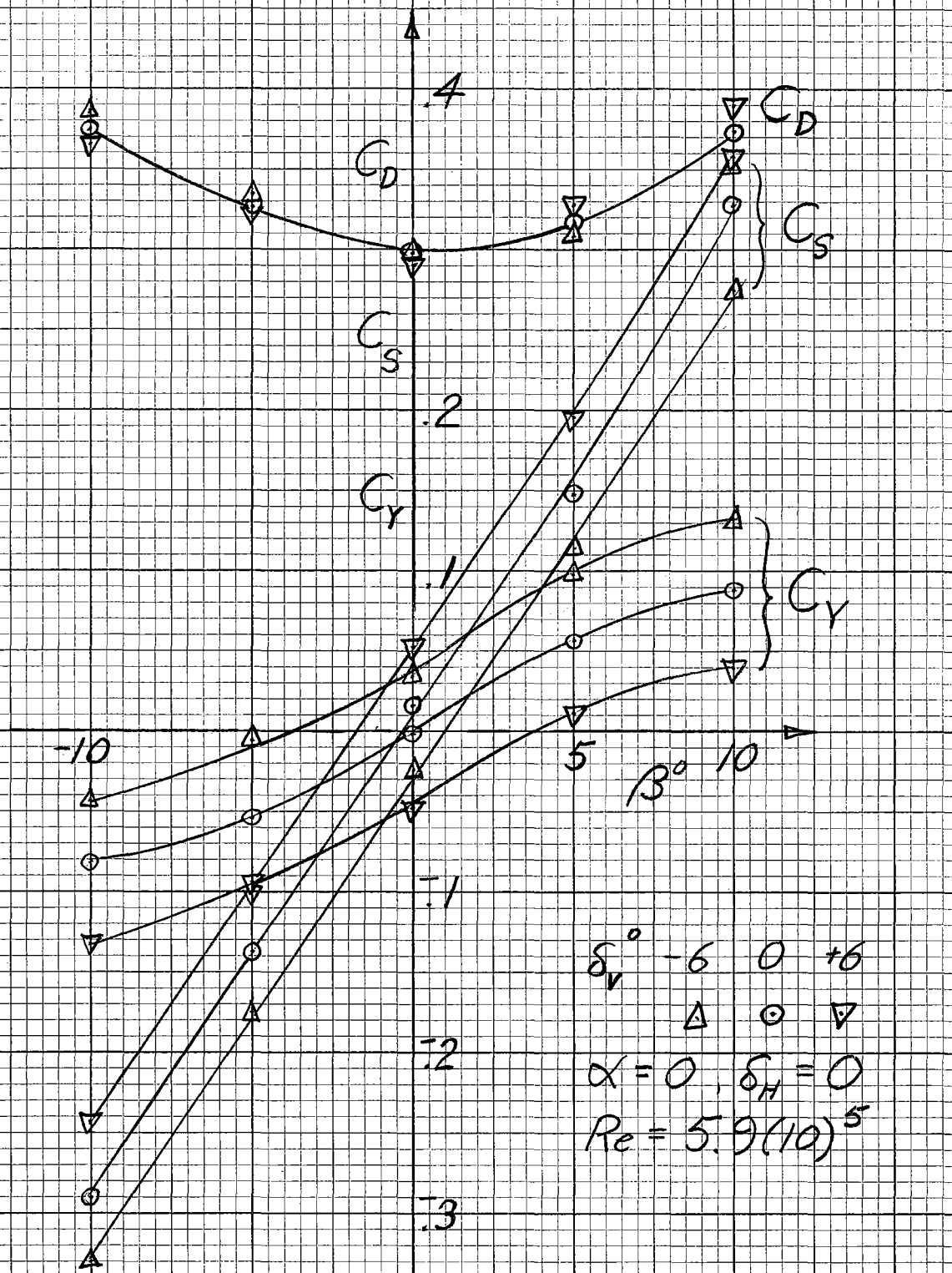

Figure 11 - Pisces IV Pitch Characteristics. Large Fins On. Nacelles Off

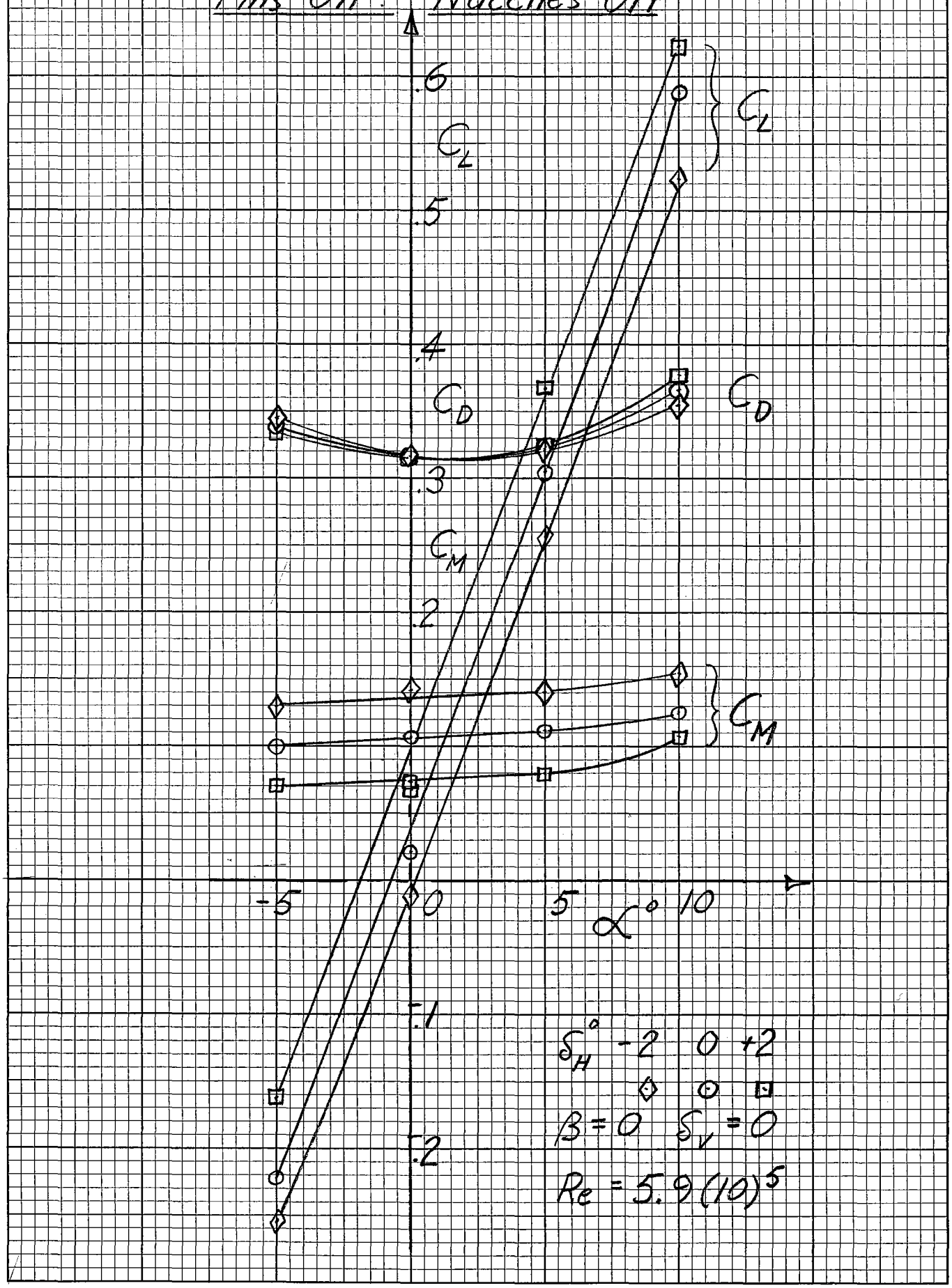

Figure 12 - Pisces IV Yaw Characteristics.
Large Fins On. Nacelles Off

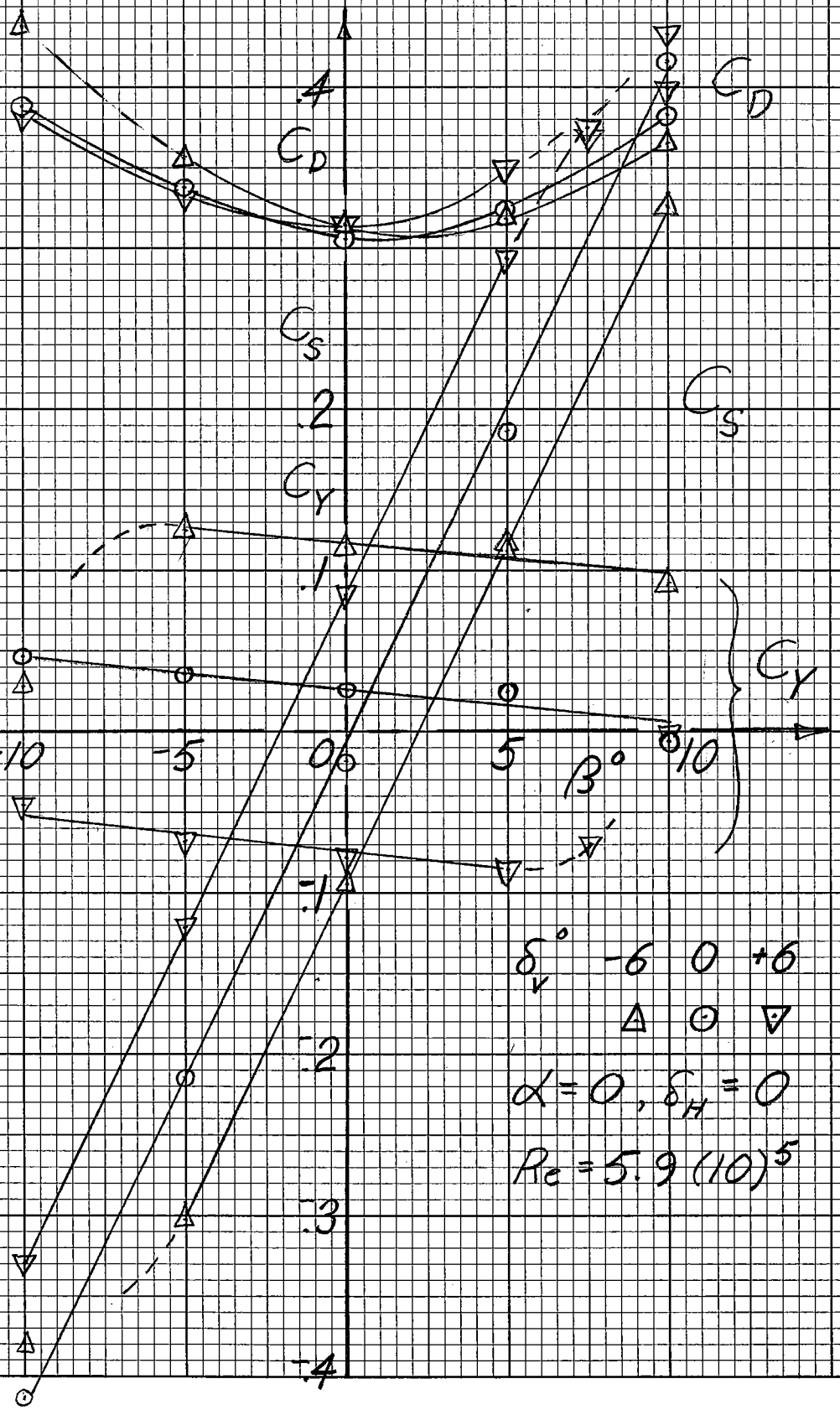

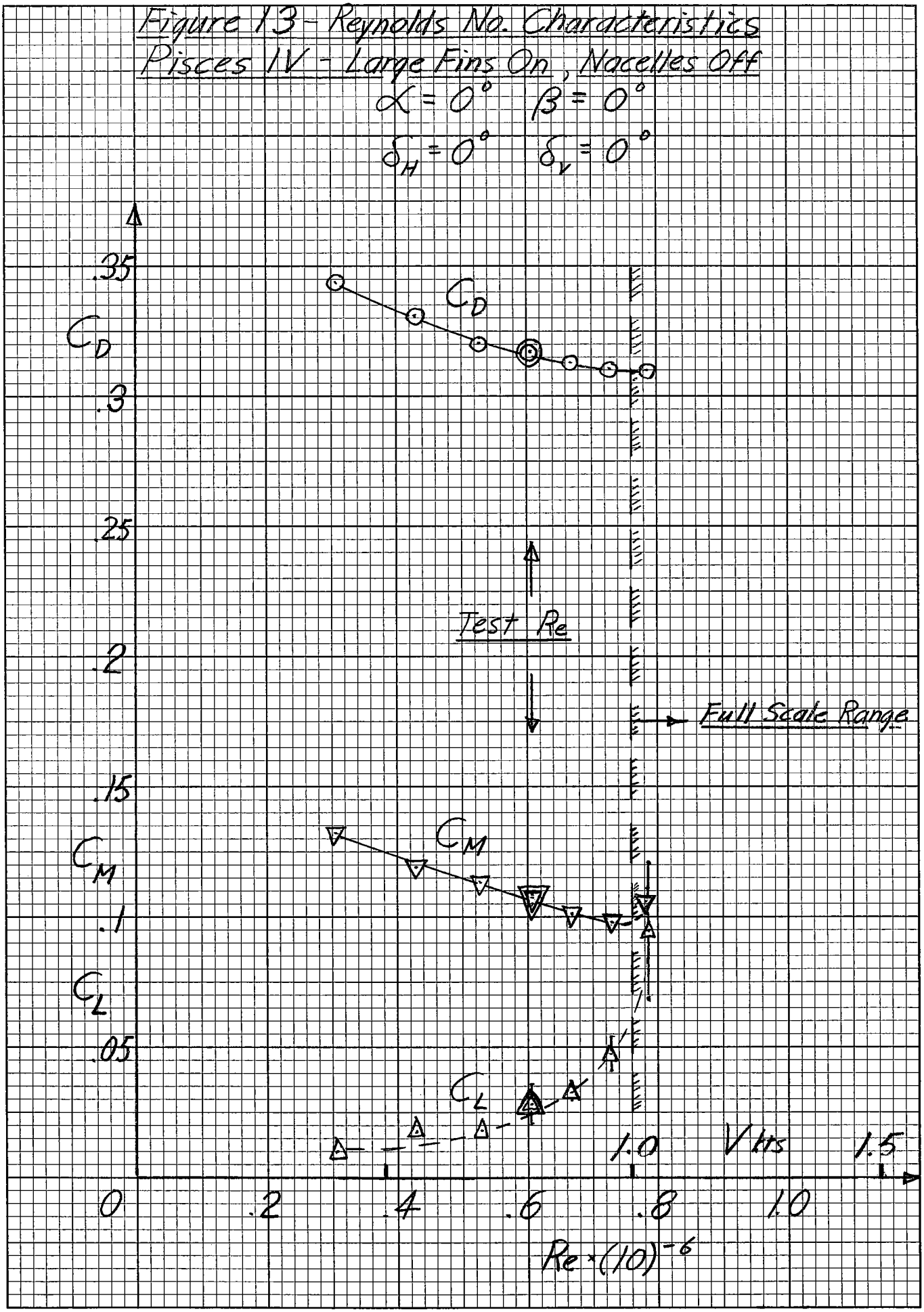
Figure 13 - Reynolds No. Characteristics
Pisces IV - Large Fins On, Nacelles Off
$\alpha = 0^\circ$ $\beta = 0^\circ$
$\delta_H = 0^\circ$ $\delta_V = 0^\circ$
C_D
.35
.3
.25
.2
.15
C_M
.1
C_L
.05
0
Test Re
Full Scale Range
C_D
C_M
C_L
.2
.4
.6
.8
1.0
1.5
2.0
V kts
Re x (10)$^{-6}$

Figure 14 - Pisces IV Control Characteristics

$\alpha = 0$ $\beta = 0$ $Re = 5.9(10)^5$

Nacelles Off

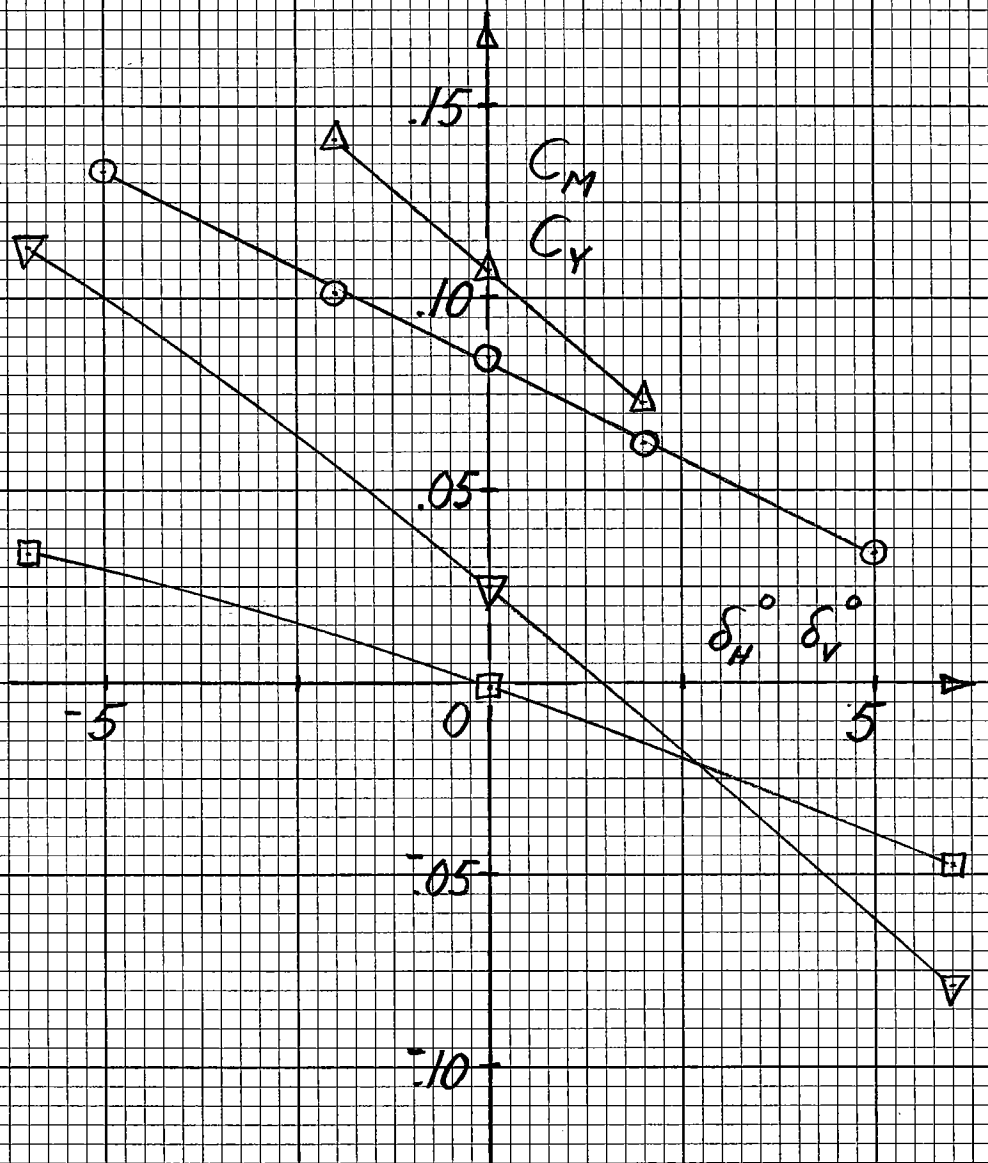

⊕ Small Fins On. C_M vs δ_H . $\delta_V = 0$

△ Large Fins On. C_M vs δ_H . $\delta_V = 0$

⊡ Small Fins On. C_Y vs δ_V . $\delta_H = 0$

▽ Large Fins On. C_Y vs δ_V . $\delta_H = 0$

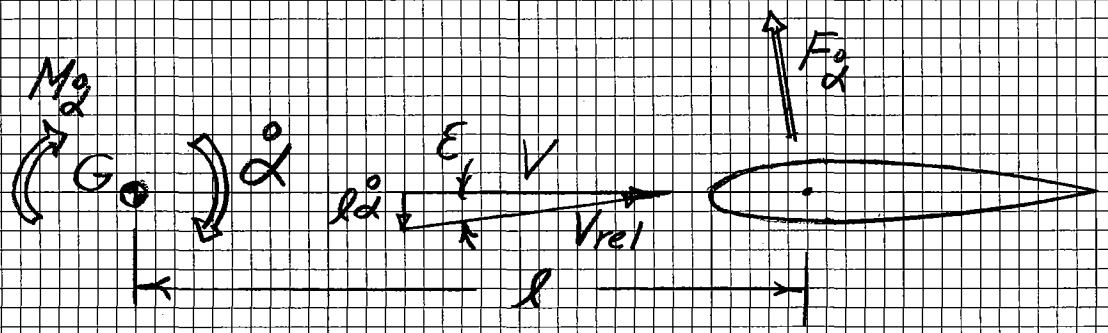

$$M_{\dot\alpha} = -F_{\dot\alpha}\,\ell\cos\varepsilon \doteq -F_{\dot\alpha}\,\ell$$
$$\varepsilon = \arctan\frac{\ell\dot\alpha}{V} \doteq \frac{\ell\dot\alpha}{V}$$
$$V_{rel} \doteq V$$
} since $\varepsilon \ll 1$

Figure 15 - Definition of Terms for Fin Pitch Damping Characteristics